

RESEARCH

Open Access



Huddling remodels gut microbiota to reduce energy requirements in a small mammal species during cold exposure

Xue-Ying Zhang^{1,2†} , Gansukh Sukhchuluun^{1,2†}, Ting-Bei Bo^{1,2†}, Qing-Sheng Chi¹, Jun-Jie Yang³, Bin Chen³, Lei Zhang^{3,4*} and De-Hua Wang^{1,2*}

Abstract

Background: Huddling is highly evolved as a cooperative behavioral strategy for social mammals to maximize their fitness in harsh environments. Huddling behavior can change psychological and physiological responses. The coevolution of mammals with their microbial communities confers fitness benefits to both partners. The gut microbiome is a key regulator of host immune and metabolic functions. We hypothesized that huddling behavior altered energetics and thermoregulation by shaping caecal microbiota in small herbivores. Brandt's voles (*Lasiopodomys brandtii*) were maintained in a group (huddling) or as individuals (separated) and were exposed to warm (23 ± 1 °C) and cold (4 ± 1 °C) air temperatures (T_a).

Results: Voles exposed to cold T_a had higher energy intake, resting metabolic rate (RMR) and nonshivering thermogenesis (NST) than voles exposed to warm T_a . Huddling voles had lower RMR and NST than separated voles in cold. In addition, huddling voles had a higher surface body temperature ($T_{surface}$), but lower core body temperature (T_{core}) than separated voles, suggesting a lower set-point of T_{core} in huddling voles. Both cold and huddling induced a marked variation in caecal bacterial composition, which was associated with the lower T_{core} . Huddling voles had a higher α and β -diversity, abundance of *Lachnospiraceae* and *Veillonellaceae*, but lower abundance of *Cyanobacteria*, *Tenericutes*, TM7, *Comamonadaceae*, and *Sinobacteraceae* than separated voles. Huddling or cold resulted in higher concentrations of short-chain fatty acids (SCFAs), particularly acetic acid and butyric acid when compared to their counterparts. Transplantation of caecal microbiota from cold-separated voles but not from cold-huddling voles induced significant increases in energy intake and RMR compared to that from warm-separated voles.

Conclusions: These findings demonstrate that the remodeling of gut microbiota, which is associated with a reduction in host T_{core} , mediates cold- and huddling-induced energy intake and thermoregulation and therefore orchestrates host metabolic and thermal homeostasis. It highlights the coevolutionary mechanism of host huddling and gut microbiota in thermoregulation and energy saving for winter survival in endotherms.

Keywords: Body temperature, Cold adaptation, Energy intake, Gut microbiota, Huddling, Thermogenesis

* Correspondence: wangdh@ioz.ac.cn

[†]Xue-Ying Zhang, Gansukh Sukhchuluun and Ting-Bei Bo contributed equally to this work.

¹State Key Laboratory of Integrated Management of Pest Insects and Rodents, Institute of Zoology, Chinese Academy of Sciences, Beijing 100101, China

²University of Chinese Academy of Sciences, Beijing 100049, China

Full list of author information is available at the end of the article



Background

Social animals and humans have evolved cooperative behaviors to maximize their fitness in harsh environments [1–3]. Among these behaviors, it has been hypothesized that huddling is one of the most acceptable benefits for species living in temperate and cold habitats to reduce thermoregulatory costs, especially in the cold season [4, 5]. Huddling mediates social thermoregulation by reducing the surface to volume ratio and, consequently, reduces heat loss and energy expenditure of the animal [6, 7]. Studies in some wild species such as the social degus (*Octodon degus*) and short-tailed field voles (*Microtus agrestis*) demonstrated that huddling reduced resting metabolic rate (RMR) and energy intake and that these metabolic advantages of huddling increased with lowered ambient temperature and increased group size [8–10].

The coevolution of mammals with their microbial communities confers fitness benefits to both partners [11–13]. Small herbivores depend mainly on caecal microbiota to digest cellulose and detoxify plant toxins [11, 14, 15]. Microbial diversity has been reported to be influenced by host physiology [16–18] and such factors as season [19–21], altitude [22], diet [23, 24], photoperiod [25], and air temperature [26, 27]. Conversely, gut microbiota, by way of their metabolites and bacterial polysaccharides, can influence host energy metabolism [26, 27], behavior [28, 29], inflammation and immunity [30–32], homeostasis of enteric and central nervous systems [33–35], and aging [36, 37]. These functions of gut microbiota have been confirmed mainly by microbiota transplantation [15, 26, 38]. Social rodent species increase the frequency of communal huddling in winter [39] and, thus, are more likely to be coprophagous. Therefore, we hypothesize that huddling may be a strong force in shaping gut microbiota and, consequently, mediate host energetics and thermoregulation.

Brandt's voles (*Lasiopodomys brandtii*), a small non-hibernating herbivorous rodent species, are widely distributed in Inner Mongolian grasslands of China, Mongolia, and Southeast Baikal region of Russia. Its habitat is characterized by extremely cold dry winter and deep frozen soil. Brandt's voles show seasonal variations in energy metabolism and thermoregulation to adapt to the seasonal environments [40, 41]. They have evolved group-living strategies such as making sounds to warn each other of predators, hoarding food collectively, and huddling to survive the cold winter. Group size in one colony increases from about 10 in summer to 20 individuals in winter [42]. However, the benefits of huddling in energy metabolism in different seasons and the underlying physiological mechanisms remain largely unknown. Here, we investigated the changes in energy intake, thermogenesis, body temperature, and gut microbiota induced by huddling in Brandt's voles in warm and cold environments, and we

transplanted microbiota to examine the hypothesis that microbiota in huddling voles can reduce energy expenditure. We demonstrated that huddling alters gut microbiota to reduce energy intake and thermoregulatory responses in a small mammal species during cold exposure.

Methods

Animal experiments

Adult Brandt's voles used in this study were from a laboratory breeding colony at the Institute of Zoology, Chinese Academy of Sciences (CAS). After weaning (at 3 weeks of age), the voles were housed with the same sex siblings at a light regime of 16-h light:8-h dark (lights on from 4:00 to 20:00) and room temperature of 23 ± 1 °C. The voles were fed a standard rabbit pellet chow (containing 18% protein, 3% fat, 12% fiber, and 47% carbohydrate, Beijing KeAo Bioscience Co.) and were provided with water ad libitum. The animal procedures were approved by the Animal Care and Use Committee of Institute of Zoology, CAS.

A total of 124 female voles (aged 4 months) were placed in 31 cages (4 voles/cage) and were divided into 4 treatments: cold (at 4 ± 1 °C) huddling (CH, 7 cages), cold separated (CS, 7 cages), warm (at 23 ± 1 °C) huddling (WH, 8 cages), and warm separated (WS, 9 cages). Sibling voles were chosen preferentially and were acclimated to the cage (42 cm \times 27 cm \times 20 cm) for 3 weeks and then to the treatment conditions for another 3 weeks. The cages contained four equal compartments separated by stainless steel walls with small holes (6 mm in diameter). Openings (7 cm \times 7 cm) in the walls allowed movement among the compartments. The openings were open for the huddling groups but closed for the separated groups, which had olfactory, visual, and vocal contacts. Individual voles were dyed on different positions of the body for identification.

Body weight and energy intake

Voies were weighed at the beginning (day 0) and the end of (day 28) of the study using an electronic balance (Sartorius Model BL 1500, ± 0.1 g), and body weight change was calculated. Food was provided ad libitum and food intake and fecal output were measured for three consecutive days in the last week of acclimation [43]. Uneaten food and feces were collected after the 3 days, oven dried at 60 °C until constant mass, and separated manually. Water content of the food offered was calculated by drying samples at 60 °C until constant mass, and its gross energy was measured by bomb calorimetry (Parr1281 Instrument, USA). Gross energy intake was calculated by subtracting the gross energy of the uneaten food from the gross energy of the food offered.

RMR and nonshivering thermogenesis (NST)

RMR, measured as oxygen consumption, was determined in huddling and separated voles at their acclimated temperatures of 4 and 23 °C at the end of the experiment. An open-circuit respirometry system (TSE labmaster, Germany) with an air flow rate of 3 L/minute was used. Voles were maintained in a 5.8 L transparent metabolic chamber (type II for rats) with double-layered meshes for the separation of voles during the measurements. The animals were allowed 1 h for acclimation to the conditions, and then recordings of O₂ uptake were taken for 2 h. An average of a minimum of three consecutive stable readings was taken as the RMR.

NST was determined on individual animals at 25 °C on the day after RMR measurements. The volume of metabolic chamber was 2.7 L (type I for mice). The voles were injected subcutaneously with norepinephrine (NE) (Shanghai Harvest Pharmaceutical Co. LTD) at a dosage of $2.53M_b^{-0.4}$ (mg/kg; M_b , body mass) [44]. NST was estimated as the four highest consecutive stable readings of oxygen consumption during 1 h.

Body temperature

In the last week of acclimation, surface body temperature (T_{surface}) was read with an infrared camera (FLIR E60, UK) from a distance of 40 cm, and the data were analyzed by FLIR Tools software [8, 26]. T_{surface} was averaged from seven to eight images for each cage. The perimeter temperature (T_p) of the voles was determined by fitting a polygon around the individual animal in the case of separated animals and around the entire group for huddling animals using the option “isotherm” of the software. The highest temperature in an image was selected as the maximum temperature (T_m). Furthermore, the contact temperature (T_c) between two animals in the huddling groups was determined by the “mobile” option.

Core body temperature (T_{core}) was recorded during the acclimation period through transponders (G2 E-Mitter, to ± 0.1 °C, STARR life sciences) implanted in the abdomen of one vole in each cage ($n = 4\text{--}5$ voles/group). The voles were anesthetized by intraperitoneal injection of pentobarbital sodium (50 mg/kg). After the abdominal skin was sterilized with iodophor, an incision of up to 1 cm in length was made below the diaphragm. The wound was closed with absorbable PGA surgical suture (Jinhuan Model R413, 4/0) and sterilized with iodophor again. The animals were allowed 10 days to recover from surgery [45]. All receivers for collecting data were connected to a computer with the Vital View software.

Short-chain fatty acids (SCFAs)

At the end of experiment, one vole from each cage (but not the one with E-Mitter) was sacrificed by CO₂ asphyxiation. The digestive tract and caecal content were

removed on a super-clean worktable, frozen immediately in liquid nitrogen, and stored at -80 °C. Six SCFAs including acetic, propionic, butyric, isobutyric, valeric, and isovaleric acids were measured in caecal contents by high-performance gas chromatography (GC, Agilent 7890A; Agilent Technologies, Germany) with a GC autosampler and a FID system by the modified method [46, 47]. Caecal contents were extracted directly with water and did not require derivatization [46, 47]. Separations were performed in a $30\text{ m} \times 0.25\text{ mm} \times 0.25\text{ }\mu\text{m}$ DB-WAX column (Agilent Technologies) using 99.998% hydrogen as carrier gas at a flow rate of 1.0 mL/min. The system was operated at 250 °C. Injections were performed in the splitless mode at 230 °C, and 0.5 μL for each injection. The oven temperature was programmed from 60 °C (1 min) to 200 °C at 5 °C/min and then from 200 to 230 °C at 10 °C/min. The total running time of each sample was 32 min.

Microbiota DNA extraction, evaluation, and amplification

DNA from caecal contents was extracted by $2 \times$ CTAB (cetyltrimethyl ammonium bromide), phenol chloroform mixture (phenol:chloroform:isoamyl alcohol = 25:24:1). In the later steps of DNA isolation, we used the spin column from SanPrep Column DNA Gel Extraction Kit (Sangon Biotech, China) (based on a silica gel membrane) to purify and recover the DNA rapidly. DNA concentration was measured by fluorometry using the Qubit® dsDNA high-sensitivity assay kit and the Qubit® 2.0 fluorometer (Life Technologies, Carlsbad, CA, USA) as instructed by the manufacturer. DNA purity was also assessed by absorbance on a Nanodrop 2000 (Thermo Fisher Scientific, Carlsbad, CA, USA) by measuring the A260/A280 ratio. Only DNAs with an A260/A280 ratio of 1.8–2.0 were used for PCR amplification ($n = 6$ voles/group). Our target was the V3–V4 hyper-variable region of the bacterial 16S rRNA gene. PCR was started immediately after the DNA was extracted. The 16S rRNA V3–V4 amplicon was amplified using $2 \times$ Taq PCR MasterMix (Tiangen, Beijing, China). Two universal bacterial 16S rRNA gene amplicon PCR primers (PAGE purified) were used: forward primer-341F (CCTACGGGNGGCWGC AG) and reverse primer-805R (GACTACHVGGGTAT CTAATCC) [48]. To multiplex the samples during sequencing, barcodes were added to the 5' termini of the forward primers (Additional file 1 Table S1). The PCR reaction was set up as follows: template DNA 2 μL , amplicon PCR forward primer (10 μM) 1 μL , amplicon PCR reverse primer (10 μM) 1 μL , and $2 \times$ Taq PCR MasterMix 12.5 μL (total 25 μL). PCR was performed for each DNA sample in triplicate in the same thermal cycler (T100™ BIO-RAD) using the following program: 1 cycle of denaturing at 94 °C for 5 min, followed by 34 cycles of denaturing at 96 °C for 30 s, annealing at 52 °C for 30 s,

elongation at 72 °C for 30 s, and a final extension at 72 °C for 5 min. The PCR products were checked using electrophoresis in 1% (*w/v*) agarose gels in TBE buffer (Tris, boric acid, EDTA) stained with ethidium bromide (EB) and visualized under UV light. PCR products were pooled and purified using Agencourt AMPure XP magnetic beads (Beckman) according to the manufacturer's instructions. Then Sequencing was done on an Illumina HiSeq 2500.

16S rRNA gene amplicon sequencing analysis

The 16S sequence paired-end data set was joined and quality filtered using the FLASH method described by Magoc and Salzberg [49]. All sequences analysis was provided in the Quantitative Insights Into Microbial Ecology (QIIME, version 1.9.1) software suite [50], according to the Qiime tutorial (<http://qiime.org/>) with some modified methods. Chimeric sequences were removed using usearch61 [51] with de novo models. Sequences were clustered against the 2013 Greengenes (13_5 release) ribosomal database's 97% reference data set. Sequences that did not match any entries in this reference were subsequently clustered into de novo OTUs at 97% similarity with UCLUST. Taxonomy was assigned to all OTUs using the RDP classifier [52] within QIIME and the Greengenes reference data set. Rarefaction and rank abundance curves were calculated from OTU tables using alpha diversity and rank abundance scripts within the QIIME pipeline. The hierarchical clustering based on population profiles of most common and abundant taxa was performed using UPGMA clustering (Unweighted Pair Group Method with Arithmetic Mean, also known as average linkage) on the distance matrix of OTU abundance. This resulted in a Newick formatted tree, which was obtained utilizing the QIIME package.

Caecal microbiota transplantation (CMT)

To remove microbiota, the healthy 4-month-old male voles were housed in separate cages at a room temperature (23 ± 1 °C) and were offered water with fresh composite antibiotics (containing 100 µg/mL neomycin, 50 µg/mL streptomycin, 100 U/mL penicillin; Sigma, Germany) for 7 days as described previously [26]. For microbiota transplantation, the caecal contents were collected from three donors each of CH, CS, and WS male voles, diluted (200 mg) in 0.9% sodium chloride injection (physiological saline, 2 mL), and then, a 200 µL suspension was delivered by intragastric gavage to each bacteria-restricted recipient vole ($n = 6$ voles/group). For the control group, saline (200 µL) was delivered by intragastric gavage to each animal. The recipients were still housed in separate cages at room temperature after CMT. Body weight and energy intake were measured during antibiotic treatment and within 1 week after CMT, and RMR and NST were determined 1 week after

CMT. After the experiment, the voles were sacrificed and caecal contents were collected for 16S rRNA sequencing ($n = 2-4$ /group) and SCFAs measurement.

Statistical analysis

The software SPSS 17.0 was used for statistical analyses. Prior to statistical analyses, all the data were examined for assumptions of normality and homogeneity of variance by Kolmogorov–Smirnov and Levene tests, respectively. The data with abnormal distribution were transformed by natural logarithms to normalize them. The data for body weight gain were transformed by arcsine and analyzed by two-way ANOVA (cold and huddling). Energy intake, RMR and NST were analyzed by two-way ANCOVA with body weight as a covariate. T_{surface} , T_{core} , the concentration of SCFAs, and microbial composition were analyzed by two-way ANOVA. Significant group differences were further evaluated using Bonferroni post hoc tests. All values were presented as mean \pm SEM (standard error of mean), and $P < 0.05$ was considered to be statistically significant.

For microbiota data, to account for any bias caused by uneven sequencing depth, the least number of sequences present in any given sample from a sample category was selected randomly prior to calculating community-wide dissimilarity measures (α -diversity and β -diversity). We rarefied the OTU table to a sequencing depth of 12,000 per sample for both diversity analyses. All principal coordinate analyses (PCoA) were based on unweighted and weighted UniFrac distances using evenly sampled OTU abundances. Significance for PCoA (β -diversity) analyses was checked with multivariate permutation tests using the nonparametric method "ADONIS" (999 permutations) included in the package "vegan" of the QIIME-incorporated version of "R". The boxplot representation of the α -diversity results was done with STAMP [53] and the calculation of P values was done with Welch's t test. The linear discriminant analysis (LDA) Effect Size (LEfSe) method was used to assess differences in microbial communities using a LDA score threshold of 2 [54].

Results

Body weight gain, energy intake, RMR, and NST

Body weight at the end (day 28) of acclimation was not affected by huddling or cold (Additional file 1 Table S2). The voles in cold air temperature (T_a) tended to gain less body weight than those in warm ($F_{1,64} = 3.467$, $P = 0.067$). Body weight gain was not affected by huddling ($F_{1,64} = 1.120$, $P = 0.294$) or the interaction between cold and huddling ($F_{1,64} = 0.174$, $P = 0.678$; Fig. 1a). Cold led to a significant increase in energy intake compared with warm condition ($F_{1,22} = 46.259$, $P < 0.001$; Fig. 1b). The huddling voles consumed less energy than separated voles in cold and warm conditions ($F_{1,22} = 28.433$, $P < 0.001$). Energy intake was

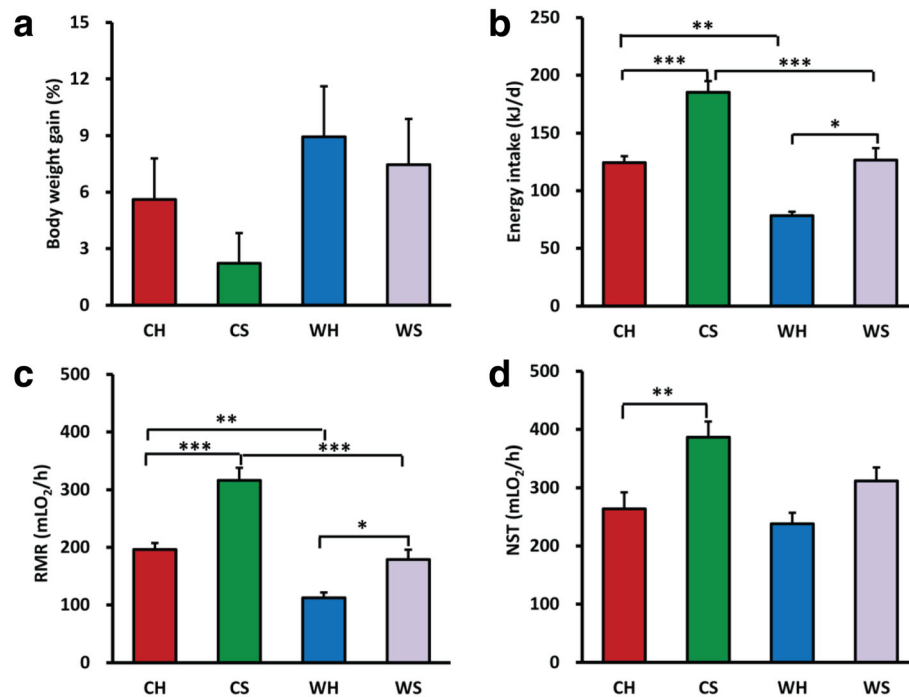


Fig. 1 Effects of huddling and cold on metabolic phenotypes. **a–d** Body weight gain, energy intake ($n = 6–8$ /group), resting metabolic rate (RMR), and nonshivering thermogenesis (NST) ($n = 7–9$ /group) in huddling and separated Brandt's voles at warm and cold air temperatures (T_a). * $P < 0.05$, ** $P < 0.01$, and *** $P < 0.001$

not affected by the interaction between cold and huddling ($F_{1,22} = 1.352$, $P > 0.05$).

At the end of experiment, huddling voles had lower RMR than separated voles ($F_{1,26} = 27.041$, $P < 0.001$; Fig. 1c). RMR was affected by cold ($F_{1,26} = 47.378$, $P < 0.001$), but was not affected by the interaction between cold and huddling ($F_{1,26} = 2.550$, $P = 0.122$). RMR of huddling voles was 37% lower than in separated ones, both in cold ($P < 0.001$) and warm T_a ($P = 0.05$) (Fig. 1c). The huddling voles also had lower NST than separated voles ($F_{1,24} = 8.458$, $P = 0.008$; Fig. 1d). NST was marginally affected by cold ($F_{1,24} = 3.815$, $P = 0.063$), but was not affected by the interaction between cold and huddling ($F_{1,24} = 0.928$, $P = 0.345$). NST of CH voles was 31% lower than CS voles ($P = 0.01$), but was not different from WH voles ($P > 0.05$) (Fig. 1d).

Body temperature

The T_{surface} including T_m and T_p was affected significantly by huddling ($P < 0.001$), cold ($P < 0.001$) and their interaction ($P < 0.05$; Fig. 2a, b). Huddling voles had higher T_m and T_p than separated voles both in warm (by 2 °C) and cold (by 3.1 °C for T_m and 4.4 °C for T_p) conditions. Cold exposure resulted in lower T_m (by 4.6 °C in huddling and by 5.8 °C in separated group) and T_p (by 8 °C in huddling and by 10.4 °C in separated group) than in warm T_a . The T_c was 7.5 °C lower in

cold huddling than in warm huddling voles ($t = 10.917$, $df = 13$, $P < 0.001$).

In the first 2 days of exposure to cold, T_{core} dropped immediately both in huddling and separated voles. The separated voles in cold increased T_{core} to the same level to the voles in warm, while the huddling voles continued to decrease T_{core} (Fig. 2c). After 10 days of exposure, the voles kept relatively stable T_{core} in cold T_a . Cold-exposed voles decreased their daily T_{core} by 1 °C compared with voles in warm T_a ($F_{1,52} = 994.295$, $P < 0.001$) (Fig. 2d, e). T_{core} was 0.3 °C lower in huddling voles than separated voles both in warm and cold conditions ($F_{1,52} = 91.581$, $P < 0.001$). The daily T_{core} was not affected by the interaction between cold and huddling ($F_{1,52} = 0.500$, $P > 0.05$).

Huddling and cold alter the diversity and composition of gut microbiota

Huddling voles had a higher phylogenetic diversity (α -diversity) than separated voles ($P = 7.85e-4$), whereas the effect of cold temperature on phylogenetic diversity was not significant ($P = 0.938$) (Fig. 3a, Additional file 1: Table S1, Additional file 1: Table S3). The PCoA of unweighted (Fig. 3b) and weighted (Fig. 3c) UniFrac distances (β -diversity) between each sample among four groups showed that the microbial communities were significantly separated by cold at the first principal

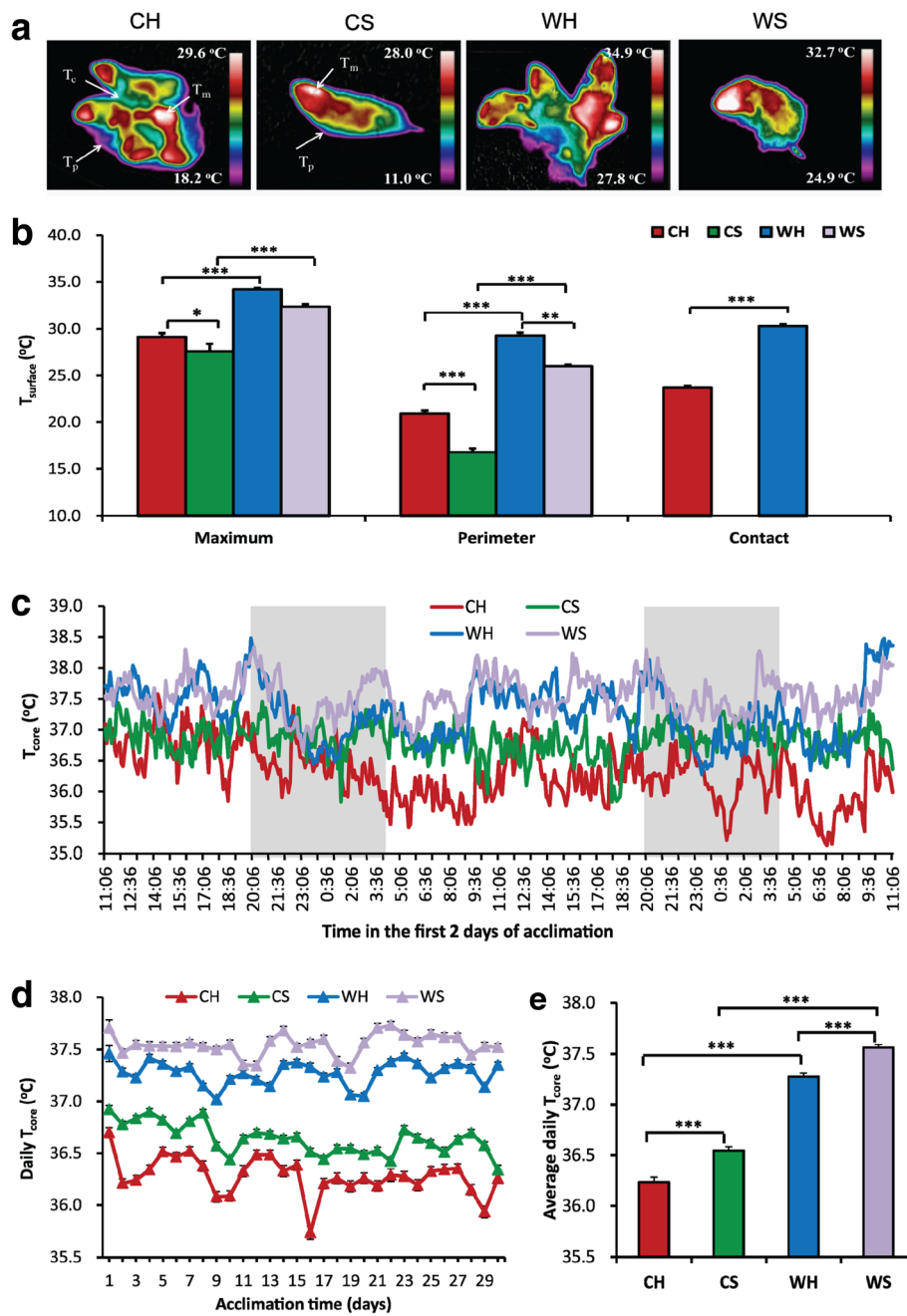


Fig. 2 Effects of huddling and cold on body temperature. **a** Infrared images of representative CH (cold huddling), CS (cold separated), WH (warm huddling), and WS (warm separated) voles ($n = 7-8$ /group) measured in the second week of acclimation. **b** $T_{surface}$ (surface body temperature) by infrared temperature readings from the eye (maximum temperature, T_m), around individual animals, or the entire groups (perimeter temperature, T_p) and between two animals only in huddling groups (contact temperature, T_c). **c** T_{core} (core body temperature) in the first 2 days of exposure ($n = 4-5$) in huddling and separated Brandt's voles at warm and cold T_a . The gray area indicated scotophase (20:00–04:00). **d, e** Average daily T_{core} ($n = 4-5$) in huddling and separated Brandt's voles at warm and cold T_a . *** $P < 0.001$

coordinate (PC1 axis) except for the WH group and also by huddling at the second principal coordinate (PC2 axis) in the cold (Fig. 3b, Additional file 1: Table S4). There were significant differences in UniFrac distances within groups ($F_{7,196} = 11.261$, $P < 0.001$; Additional file 1:

Figure S2). Intergroup UniFrac distances were markedly higher than intragroup distances ($P < 0.001$), indicating distinctive microbial community structures in each group. The intragroup distances were significantly affected by huddling ($F_{1,56} = 4.903$, $P = 0.031$) and the

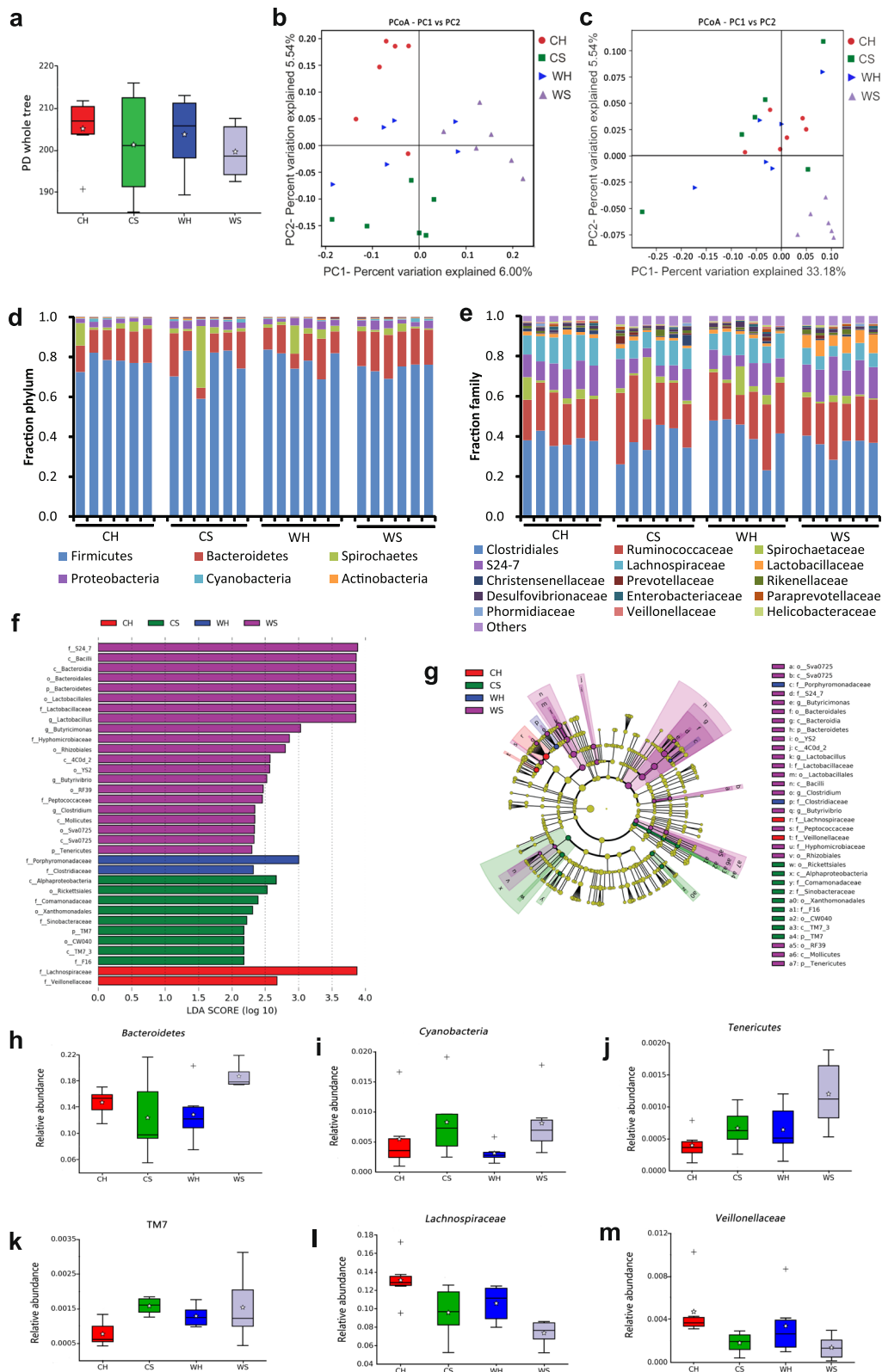


Fig. 3 (See legend on next page.)

(See figure on previous page.)

Fig. 3 Both huddling and cold alter the diversity and composition of caecal microbiota. **a** Phylogenetic diversity (PD)—whole tree analysis for the samples from CH (cold huddling), CS (cold separated), WH (warm huddling), and WS (warm separated) voles after 3 weeks of acclimation. **b, c** Principal coordinates analysis (PCoA) plots based on unweighted and weighted UniFrac distance. Each symbol represents a single sample of caecal contents from the four groups. **d, e** Relative abundance at phylum and family levels in caecal microbiota community of the four groups. **f** Differential bacterial taxonomy selected by LEfSe analysis with LDA score > 2 in caecal microbiota community of the four groups. **g** Cladogram representing taxa enriched in caecal microbiota community of the four groups detected by the LEfSe tool. Differences were represented by the color of the most abundant class (red indicating CH group, green CS group, blue WH group, purple WS group, and yellow non-significant). The diameter of each circle is proportional to the taxon's abundance. **h–m** Relative abundance of *Bacteroidetes*, *Cyanobacteria*, *Tenericutes*, TM7, *Lachnospiraceae*, and *Veillonellaceae* in caecal microbiota community of the four groups. In panels **a** and **h–m**, the white star indicates the mean of data, and the whisker indicates the most extreme data point within 1.5*(75th–25th percentile) of the median. Data points outside of the whiskers are shown as crosses

interaction of huddling and cold ($F_{1,56} = 11.461$, $P = 0.001$), but not affected by cold ($F_{1,56} = 0.976$, $P = 0.328$).

Analysis at the phylum level showed that the dominant phyla (mean relative abundance > 1%) in voles included *Firmicutes* (76.9%) and *Bacteroidetes* (13.6%). Rare phyla included *Spirochaetes* (4.9%), *Proteobacteria* (3.2%), *Cyanobacteria* (0.6%), *Actinobacteria* (0.4%), and TM7 (0.1%) (Fig. 3d). Analysis at the family level showed that the dominant six families were *Clostridiales* (38.7%), *Ruminococcaceae* (23.1%), S24–7 (11.1%), *Lachnospiraceae* (10.9%), *Spirochaetaceae* (4.9%), and *Lactobacillaceae* (1.9%) (Fig. 3e).

To assess differences in microbial communities affected by huddling and cold, we applied LEfSe method with LDA score > 2 (Fig. 3f, g). The results identified 2 discriminative features in the microbiota of CH voles, 9 in CS, 2 in WH, and 21 in WS voles. Huddling induced major shifts of the microbiota composition, with significant decreases in proportions of *Cyanobacteria*, *Tenericutes* and TM7 at the phylum level, and of RF39, *Rickettsiales*, *Comamonadaceae*, and *Sinobacteraceae* at the order or family level, but increases in *Lachnospiraceae* and *Veillonellaceae* when compared with the separated voles (Fig. 3f, h–m, Additional file 1: Table S5). The proportions of *Tenericutes*, RF39, *Lactobacillaceae*, *Peptococcaceae*, and *Clostridiaceae* were lower, but of *Lachnospiraceae* were higher in cold voles than in warm voles. The proportions of *Bacteroidetes* were affected by the interaction of cold and huddling and were higher in CH and WS groups than in CS and WH groups.

Huddling and cold alter microbial metabolites

The huddling voles increased acetic acid concentration in cold ($F_{1,26} = 6.256$, $P = 0.019$), but decreased isovaleric acid concentration in warm ($F_{1,26} = 6.311$, $P = 0.019$) when compared with separated voles (Fig. 4). Cold exposure induced increases in the concentrations of acetic acid in huddling voles ($F_{1,26} = 4.649$, $P = 0.041$) and butyric acid in separated voles ($F_{1,26} = 4.588$, $P = 0.042$) when compared with warm conditions. The concentrations of propionic acid, isobutyric acid, and valeric acid

were not affected by cold or huddling ($P > 0.05$). Total SCFAs were higher in cold than those in warm ($F_{1,26} = 5.293$, $P = 0.030$) and in huddling than those in separated voles ($F_{1,26} = 5.710$, $P = 0.024$). The isovaleric acid concentration was affected by the interaction between cold and huddling ($F_{1,26} = 5.094$, $P = 0.033$).

CMT alters energy metabolism, gut microbiota, and microbial metabolites

There was no difference in body weight among all groups during antibiotic treatment ($F_{3,20} = 0.038$, $P = 0.990$) or after CMT ($F_{3,20} = 0.135$, $P > 0.05$; Fig. 5a). Energy intake among groups did not differ during antibiotic treatment ($F_{3,19} = 0.253$, $P = 0.871$), but CMT from

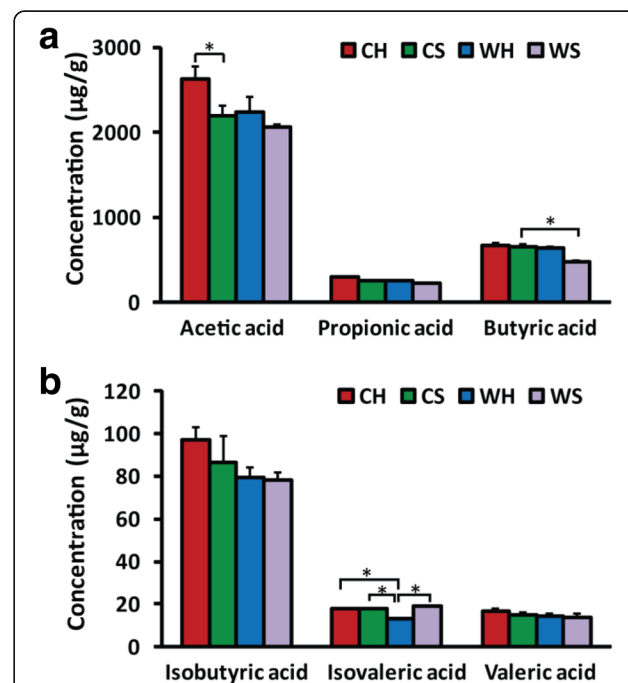


Fig. 4 Effects of huddling and cold on the concentrations of short-chain fatty acids (SCFAs). The concentrations of acetic acid (a), propionic acid (b), butyric acid (c), isobutyric acid (d), valeric acid (e), and isovaleric acid (f) in huddling and separated Brandt's voles at warm and cold T_a ($n = 7–9$ /group). * $P < 0.05$

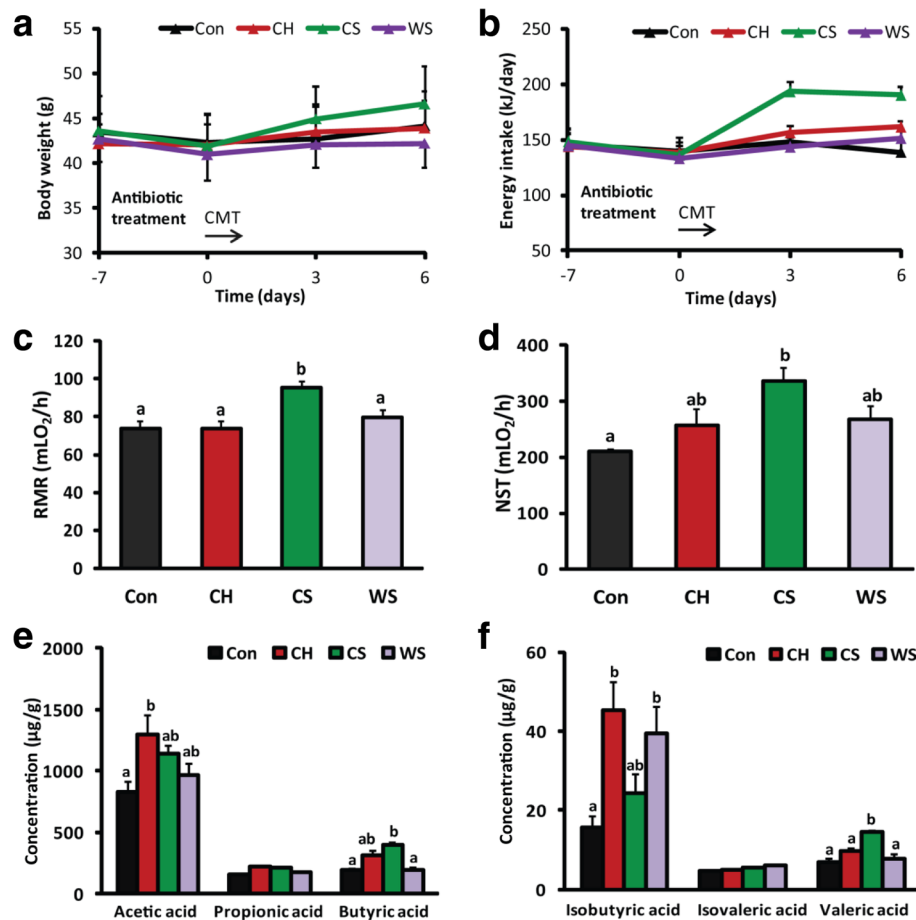


Fig. 5 Caecal microbiota transplantation (CMT) affects energy metabolism and microbial metabolites. **a** There was no difference in body weight before or after CMT among groups ($n = 6/\text{group}$). **b** CS microbiota increased energy intake compared with CH and WS microbiota and Con (saline) after 3 days of CMT. There was no difference in energy intake among Con, CH, and WS groups. **c** CS rather than CH microbiota increased RMR compared with saline (Con) and WS microbiota. **d** CS rather than CH microbiota increased NST compared with Con voles. **e, f** CMT resulted in significant changes in the concentrations of acetic acid, butyric acid, isobutyric acid, and valeric acid among groups. Bars not sharing common letters indicate a significant difference ($P < 0.05$)

CS voles led to an increase in energy intake at day 3 ($F_{3,19} = 10.253$, $P < 0.001$) and day 6 ($F_{3,19} = 8.914$, $P = 0.001$; Fig. 5b) compared to the other groups. The voles transplanted with CS microbiota had higher RMR than the other three groups ($F_{3,19} = 6.688$, $P = 0.003$; Fig. 5c) and also had higher NST than the control group ($F_{3,19} = 5.001$, $P = 0.010$; Fig. 5d).

CMT resulted in significant changes in the concentrations of acetic acid ($F_{3,20} = 3.802$, $P = 0.026$), butyric acid ($F_{3,20} = 4.265$, $P = 0.018$), isobutyric acid ($F_{3,20} = 5.909$, $P = 0.005$), and valeric acid ($F_{3,20} = 7.910$, $P = 0.001$) among groups (Fig. 5e, f). Voles transplanted with CS microbiota had higher concentrations of butyric acid and valeric acid than the other groups ($P < 0.05$; Fig. 5e, f).

The data of 16S rRNA sequencing showed that antibiotic treatment and microbiota transplantation markedly altered microbial quantity as assessed by

Shannon, chao1, observed OTUs, and PD whole tree (α -diversity, Additional file 1: Figure S3) and altered microbial community composition measured by unweighted UniFrac distances (β -diversity, Additional file 1: Figure S4 a–c). Group differences in microbial communities affected by antibiotic treatment and microbiota transplantation were found by LEfSe method with LDA score > 2 (Additional file 1: Figure S4 d). We also observed that the recipients (R) had the similar abundance of biomarkers as the donors (D) in the respective groups (Additional file 1: Figure S4 e–j).

Discussion

Huddling is a social thermoregulatory behavior in mitigating cold stress in endotherms. In the present study, we investigated the underlying coevolutionary and physiological mechanisms of huddling in regulating

energy intake and thermogenesis from the new aspect of gut microbiota. We observed that huddling voles had higher T_{surface} but lower T_{core} than voles that could not huddle (separated). Huddling also resulted in decreases in energy intake, RMR, and NST in both warm and cold T_a . Both cold and huddling resulted in marked alterations in caecal bacterial composition at the phylum and family levels and also significant changes in microbial metabolites. Further, CMT indicated that huddling- or cold-induced variations in caecal microbiota regulate energy intake and metabolic rate of the host. These results suggest that the alteration in core temperature in the gut by huddling or cold may affect bacterial growth and activity and, hence, induce the observed changes in energy intake and thermoregulation.

Huddling reduced metabolic costs

To maintain normal body temperature under cold T_a , mammals use many physiological mechanisms, including increased heat production, heat conservation, and energy intake [55]. In small mammals, RMR and NST increased during cold exposure in Brandt's voles [41, 56], prairie voles (*Microtus ochrogaster*) [57], and root voles (*Microtus oeconomus*) [58]. In the present study, although cold exposure induced an increase in RMR, huddling voles had a lower RMR than separated voles both at 4 and 23 °C. There is a lower RMR in huddling than in separated animals in many other wild mammals, such as social degus [8], short-tailed field voles [9], bank voles (*Clethrionomys glareolus*) [59], townsend's voles (*Microtus townsendii*) [60], and African four-striped grass mice (*Rhabdomys pumilio*) [61]. Besides the lower RMR, the huddling voles did not increase NST in the cold indicating an effective social behavior for heat conservation in small mammals.

Due to the lower energy expenditure, the huddling voles consumed less energy than separated voles in both cold and warm T_a . This was consistent with previous studies in mice (*Mus musculus*) [62], golden mice (*Ochrotomys nuttalli*) [63], furred Siberian hamsters (*Phodopus sungorus*) [64], and social degus at low T_a [8]. In contrast to warm T_a , however, the voles in cold would gain less body weight and/or body fat (data not shown) due to high metabolic costs, which was also found in the previous studies in voles [41, 43]. The thermoneutral zone of Brandt's vole ranges between 27.5 and 32.5 °C [65] and, therefore, the warm T_a of 23 °C used in this experiment was below the lower critical temperature. Therefore, huddling in warm group also had an energetic benefit.

Huddling increased T_{surface} but decreased T_{core}

Maintenance of high and constant T_{core} over a wide range of T_a is a high evolutionary feature of endotherms

[66]. Huddling animals reduce their thermal conductance in cold through the reduced surface to volume ratio. In addition, the contact increases skin thickness in the area of contact and thus heat transfers between voles with less loss to the environment [9, 67]. The decrease in thermal conductance in huddling animals may reduce temperature loss to the environment and thus result in higher T_{surface} compared with separated animals. Further, the increased T_{surface} as warm resources may attract voles to huddle, especially in the cold.

We found that huddling voles had a lower T_{core} than separated voles, and CH voles had the lowest T_{core} among the four groups. A similar result of lower T_{core} under huddling has been recorded in birds where the goslings of greater snow geese (*Chen caerulescens atlantica*) in cold arctic environments had a T_{core} by 0.3 °C when huddling [68], and emperor penguin decreased T_{core} by 0.9 °C and increased local T_{surface} during huddling in pair period in Antarctic winters [69]. We assumed that, during huddling, the voles were resting and reduced their vigilance and control system of internal heat balance, which also allowed a gradual decrease in T_{core} to the possible minimum set-point of body temperature. Moreover, the decrease in T_{core} in response to a low T_a supports the importance of sensors of the thermal environment in determining the set-point to which T_{core} is regulated [70]. Other explanations for decreased T_{core} in huddling mostly came from the reduced metabolic rate in the present study and from previous studies [68, 69]. These data indicate that huddling contributes to the reduced set-point of T_{core} and temperature gradient between T_{core} and T_{surface} to reduce individual internal heat loss and conserve energy.

Huddling shaped the diversity of caecal microbiota

Gut microbial diversity is vulnerable to the environments of wild mammals. For example, seasonal variations in gut microbial diversity were reported in wild wood mice (*Apodemus sylvaticus*) [19], ground squirrels (*Ictidomys tridecemlineatus*) [20], and wild black howler monkeys (*Alouatta pigra*) [21]. Gut microbiota also changed its diversity with different altitudes and diet diversity in plateau pikas (*Ochotona curzoniae*) [22], yaks (*Bos grunniens*), and Tibetan sheep (*Ovis aries*) [71]. We observed that huddling significantly increased the diversity of caecal microbiota compared with separated condition. Both cold and huddling could induce marked changes in caecal bacterial composition at the phylum and family levels, while huddling decreased the abundance of *Cyanobacteria*, *Tenericutes*, TM7, *Comamonadaceae*, and *Sinobacteraceae*. Most of these are pathogenic bacteria and have been found to be associated with host inflammatory mucosal diseases [72, 73]. Moreover, huddling increased the abundance of

Lachnospiraceae and *Veillonellaceae*. The family *Lachnospiraceae* has been linked to protection from colon cancer mainly due to the production of butyric acid [74, 75]. The increased abundance of *Veillonellaceae* was previously found in the intestinal microbiota of breast-fed infants [76] and in human type 2 diabetes following prebiotic fiber intake [77], implying a beneficial effect due to the production of acetate and propionate. Therefore, these data indicate that huddling may shape the hosts to develop a healthier gut microbial community.

The shifts in caecal microbiota were associated with a reduction in T_{core} during cold exposure and in huddling in Brandt's voles. Hibernating mammals exhibit an annual temperature rhythm [78, 79] and alter the diversity and composition of gut microbiota over the circannual hibernation cycle [20, 80]. Most mammals such as mice, desert hamsters (*Phodopus roborovskii*), and even humans show daily body temperature rhythm [81, 82] and the diurnal variation of gut microbiota has been reported in mice [83, 84]. A recent study showed that a 2–3 °C increase in ambient temperature can cause a 34% loss in gut bacterial diversity in a vertebrate ectotherm, the common lizard (*Zootoca vivipara*) [85]. Although there is still no direct evidence about the relationship between the host body temperature and gut microbiota in mammals, it is possible that a reduced core temperature in the gut may change bacterial growth and activity and, hence, the observed changes in gut microbial community.

Gut microbiota regulates energy intake and thermogenic capacity of the host

Microbial metabolites, by interacting with enteric nervous system, provide the causal links between

environment-induced alterations in gut microbiota and the physiological and behavioral responses of the host [32, 86]. We observed that the alteration in caecal microbiota was followed by changes in their metabolites. Cold exposure induced increases in concentrations of acetic acid in huddling voles and butyric acid in separated voles. A number of data indicated that the principal products of caecal fermentation of dietary fiber, such as acetic, butyric, and propionic acids, by acting on the free fatty acid receptors (FFAR2 and FFAR3, previously named G-protein-coupled receptors GPR43 and GPR41) contributed to regulating the release of anorexigenic hormones peptide YY (PYY) and glucagon-like peptide (GLP)-1 from the gut [87, 88] and leptin secretion from adipocytes [89], and controlled appetite, energy intake, and thermogenesis [90–92]. Thus, the increased SCFAs, particularly acetic acid and butyric acid in cold and/or huddling animals, help maintain metabolic and thermal homeostasis.

In the present study, the changes in energy intake, RMR and NST were accompanied by variations in caecal microbiota during cold exposure and during huddling. In addition, the voles transplanted with CH microbiota had a lower energy intake and RMR than voles transplanted with CS microbiota, confirming that gut microbiota regulated energy intake and metabolic rate of the host. Further support was provided by the findings that cold microbiota transplanted to germ-free mice led to an increase in white fat browning and energy expenditure [26, 27]. The concentrations of SCFAs also showed that CMT altered microbial metabolites, as CS microbiota increased the concentrations of acetic acid and butyric acid. These

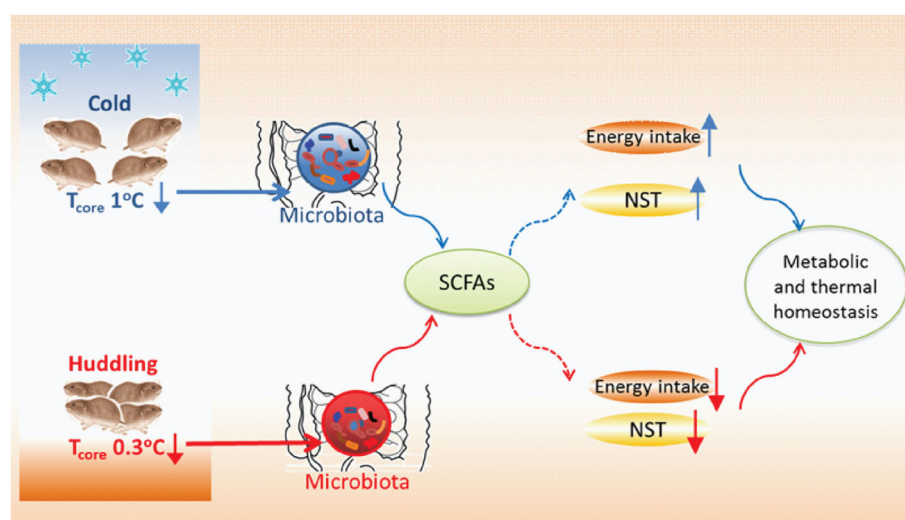


Fig. 6 Schematic model that cold- or huddling-induced remodeling of gut microbiota orchestrates host metabolic and thermal homeostasis. SCFAs, short-chain fatty acids; NST, nonshivering thermogenesis

data provide further support for microbial functioning as a potential player in the shifted host metabolic physiology.

Conclusion

For the first time, the current study presents new insight into the coevolutionary mechanism of host huddling and gut microbiota in thermoregulation and energy saving for winter survival in endotherms. Huddling voles reduced energy intake and conserved energy by reducing metabolic rate and set-point of T_{core} . A healthier gut microbial community was detected in huddling than in separated voles which produced more SCFAs, particularly in cold T_a . Furthermore, CMT induced the alteration in energy intake, metabolic rate, microbial communities, and metabolites. These data demonstrate that the environment-associated reduction in host T_{core} may change the gut microbial community, and the remodeling of gut microbiota and their metabolites mediate cold- and huddling-induced energy intake and thermoregulation and therefore orchestrates host metabolic and thermal homeostasis (Fig. 6).

Additional file

Additional file 1: Supplementary figures and tables. (DOC 1820 kb)

Acknowledgements

We appreciate the constructive comments and suggestions by the anonymous reviewers. We especially thank Prof. Allan Degen at Blaustein Institutes for Desert Research, Ben-Gurion University of the Negev, Israel, for his valuable comments. We also thank all members of Animal Physiological Ecology Group, Institute of Zoology of the Chinese Academy of Sciences, for discussion about this study.

Funding

This work was supported by the National Natural Scientific Foundation of China (Nos. 31770440, 31772461, and 31470474), the Beijing Natural Science Foundation (5172024), and the CAS-TWAS President's Fellowship Program (GS).

Authors' contributions

XYZ and DHW designed the study. XYZ, GS, and TBB performed the measurements and data analysis. QSC assisted with measurements of metabolic rate and body temperature. XYZ, TBB, JY, BC, and LZ measured and analyzed caecal microbiota. XYZ wrote the manuscript. All authors have read and critically revised the manuscript.

Competing interests

The authors declare that they have no competing interests.

Publisher's Note

Springer Nature remains neutral with regard to jurisdictional claims in published maps and institutional affiliations.

Author details

¹State Key Laboratory of Integrated Management of Pest Insects and Rodents, Institute of Zoology, Chinese Academy of Sciences, Beijing 100101, China. ²University of Chinese Academy of Sciences, Beijing 100049, China. ³College of Life Science, Shandong Normal University, Ji'nan 250014, China. ⁴Microbiome Research Center, Shandong Institutes for Food and Drug Control, Ji'nan 250101, China.

Received: 14 November 2017 Accepted: 9 April 2018

Published online: 08 June 2018

References

1. Franco M, Contreras C, Cortes P, Chappell MA, Soto-Gamboa M, Nespolo RF. Aerobic power, huddling and the efficiency of torpor in the South American marsupial, *Dromiciops gliroides*. *Biol open*. 2012;1(12):1178–84.
2. Vickery WL, Millar JS. The energetics of huddling by endotherms. *Oikos*. 1984;43(1):88–93.
3. Cornwallis CK, Botero CA, Rubenstein DR, Downing PA, West SA, Griffin AS. Cooperation facilitates the colonization of harsh environments. *Nat Ecol Evol*. 2017;1(3):57.
4. Glancy J, Gross R, Stone JV, Wilson SP. A self-organising model of thermoregulatory huddling. *PLoS Comput Biol*. 2015;11(9):e1004283.
5. Ebensperger LA. A review of the evolutionary causes of rodent group-living. *Acta Theriol*. 2001;46(2):115–44.
6. Gilbert C, McCafferty D, Le Maho Y, Martrette JM, Giroud S, Blanc S, et al. One for all and all for one: the energetic benefits of huddling in endotherms. *Biol Rev*. 2010;85(3):545–69.
7. Boratynski JS, Willis CK, Jefimow M, Wojciechowski MS. Huddling reduces evaporative water loss in torpid Natterer's bats, *Myotis nattereri*. *Comp Biochem Physiol A Mol Integr Physiol*. 2015;179:125–32.
8. Nunez-Villegas M, Bozinovic F, Sabat P. Interplay between group size, huddling behavior and basal metabolism: an experimental approach in the social degu. *J Exp Biol*. 2014;217(6):997–1002.
9. Hayes JP, Speakman JR, Racey PA. The contributions of local heating and reducing exposed surface-area to the energetic benefits of huddling by short-tailed field voles (*Microtus agrestis*). *Physiol Zool*. 1992;65(4):742–62.
10. Canals M, Rosenmann M, Bozinovic F. Geometrical aspects of the energetic effectiveness of huddling in small mammals. *Acta Theriol*. 1997;42(3):321–8.
11. Ley RE, Hamady M, Lozupone C, Turnbaugh PJ, Ramey RR, Bircher JS, et al. Evolution of mammals and their gut microbes. *Science*. 2008;320(5883):1647–51.
12. Ley RE, Lozupone CA, Hamady M, Knight R, Gordon JL. Worlds within worlds: evolution of the vertebrate gut microbiota. *Nat Rev Microbiol*. 2008;6(10):776–88.
13. Savage DC. Microbial ecology of the gastrointestinal tract. *Annu Rev Microbiol*. 1977;31:107–33.
14. Pennisi E. How do gut microbes help herbivores? Counting the ways. *Science*. 2017;355(6322):236.
15. Kohl KD, Weiss RB, Cox J, Dale C, Dearing MD. Gut microbes of mammalian herbivores facilitate intake of plant toxins. *Ecol Lett*. 2014;17(10):1238–46.
16. Ridaura VK, Faith JJ, Rey FE, Cheng JY, Duncan AE, Kau AL, et al. Gut microbiota from twins discordant for obesity modulate metabolism in mice. *Science*. 2013;341(6150):1079–U49.
17. Koren O, Goodrich JK, Cullender TC, Spor A, Laitinen K, Backhed HK, et al. Host remodeling of the gut microbiome and metabolic changes during pregnancy. *Cell*. 2012;150(3):470–80.
18. Sommer F, Stahlman M, Ilkayeva O, Arnemo JM, Kindberg J, Josefsson J, et al. The gut microbiota modulates energy metabolism in the hibernating brown bear *Ursus arctos*. *Cell Rep*. 2016;14(7):1655–61.
19. Maurice CF, Knowles SCL, Ladau J, Pollard KS, Fenton A, Pedersen AB, et al. Marked seasonal variation in the wild mouse gut microbiota. *ISME J*. 2015;9(11):2423–34.
20. Carey HV, Walters WA, Knight R. Seasonal restructuring of the ground squirrel gut microbiota over the annual hibernation cycle. *Am J Phys*. 2013;304(1):R33–42.
21. Amato KR, Leigh SR, Kent A, Mackie RI, Yeoman CJ, Stumpf RM, et al. The gut microbiota appears to compensate for seasonal diet variation in the wild black howler monkey (*Alouatta pigra*). *Microb Ecol*. 2015;69(2):434–43.
22. Li H, Li TT, Beasley DE, Hedenec P, Xiao ZS, Zhang SH, et al. Diet diversity is associated with beta but not alpha diversity of pika gut microbiota. *Front Microbiol*. 2016;7:1169.
23. Subramanian S, Huq S, Yatsunencko T, Haque R, Mahfuz M, Alam MA, et al. Persistent gut microbiota immaturity in malnourished Bangladeshi children. *Nature*. 2014;510(7505):417–21.
24. Ussar S, Griffin NW, Bezy O, Fujisaka S, Vienberg S, Softic S, et al. Interactions between gut microbiota, host genetics and diet modulate the predisposition to obesity and metabolic syndrome. *Cell Metab*. 2016;23(3):564–6.
25. Bailey MT, Walton JC, Dowd SE, Weil ZM, Nelson RJ. Photoperiod modulates gut bacteria composition in male Siberian hamsters (*Phodopus sungorus*). *Brain Behav Immun*. 2010;24(4):577–84.

26. Chevalier C, Stojanovic O, Colin DJ, Suarez-Zamorano N, Tarallo V, Veyrat-Durebex C, et al. Gut microbiota orchestrates energy homeostasis during cold. *Cell*. 2015;163(6):1360–74.
27. Zietak M, Kovatcheva-Datchary P, Markiewicz LH, Stahlman M, Kozak LP, Backhed F. Altered microbiota contributes to reduced diet-induced obesity upon cold exposure. *Cell Metab*. 2016;23(6):1216–23.
28. Zheng P, Zeng B, Zhou C, Liu M, Fang Z, Xu X, et al. Gut microbiome remodeling induces depressive-like behaviors through a pathway mediated by the host's metabolism. *Mol Psychiatry*. 2016;21(6):786–96.
29. Hoban AE, Stilling RM, MM G, Moloney RD, Shanahan F, Dinan TG, et al. Microbial regulation of microRNA expression in the amygdala and prefrontal cortex. *Microbiome*. 2017;5(1):102.
30. Kim HJ, Li H, Collins JJ, Ingber DE. Contributions of microbiome and mechanical deformation to intestinal bacterial overgrowth and inflammation in a human gut-on-a-chip. *PNAS*. 2016;113(1):E7–E15.
31. Strober W. Impact of the gut microbiome on mucosal inflammation. *Trends Immunol*. 2013;34(9):423–30.
32. Thaiss CA, Zmora N, Levy M, Elinav E. The microbiome and innate immunity. *Nature*. 2016;535(7610):65–74.
33. Kabouridis PS, Lasrado R, McCallum S, Chng SH, Snippet HJ, Clevers H, et al. Microbiota controls the homeostasis of glial cells in the gut lamina propria. *Neuron*. 2015;85(2):289–95.
34. Yano JM, Yu K, Donaldson GP, Shastri GG, Ann P, Ma L, et al. Indigenous bacteria from the gut microbiota regulate host serotonin biosynthesis. *Cell*. 2015;161(2):264–76.
35. Goyal MS, Venkatesh S, Milbrandt J, Gordon JI, Raichle ME. Feeding the brain and nurturing the mind: linking nutrition and the gut microbiota to brain development. *PNAS*. 2015;112(46):14105–12.
36. Han B, Sivaramakrishnan P, Lin CJ, Neve IAA, He J, Tay LWR, et al. Microbial genetic composition tunes host longevity. *Cell*. 2017;169(7):1249–62. e13
37. Heintz C, Mair W. You are what you host: microbiome modulation of the aging process. *Cell*. 2014;156(3):408–11.
38. Li SS, Zhu A, Benes V, Costea PI, Hercog R, Hildebrand F, et al. Durable coexistence of donor and recipient strains after fecal microbiota transplantation. *Science*. 2016;352:586–9.
39. McShae WJ. Social tolerance and proximate mechanisms of dispersal among winter groups of meadow voles. *Anim Behav*. 1990;39:346–51.
40. Li XS, Wang DH. Regulation of body weight and thermogenesis in seasonally acclimatized Brandt's voles (*Microtus brandti*). *Horm Behav*. 2005;48(3):321–8.
41. Zhang XY, Wang DH. Energy metabolism, thermogenesis and body mass regulation in Brandt's voles (*Lasiopodomys brandtii*) during cold acclimation and rewarming. *Horm Behav*. 2006;50(1):61–9.
42. Zhang J, Zhong WQ. On the colonial structure of Brandt's vole in burrow units. *Acta Theriol Sin*. 1981;1(1):51–6.
43. Zhang XY, Wang DH. Thermogenesis, food intake and serum leptin in cold-exposed lactating Brandt's voles *Lasiopodomys brandtii*. *J Exp Biol*. 2007; 210(3):512–21.
44. Wang JM, Wang DH. Comparison of nonshivering thermogenesis induced by dosages of norepinephrine from 3 allometric equations in Brandt's voles (*Lasiopodomys brandtii*). *Acta Theriol Sin*. 2006;26:84–8.
45. Chi QS, Wang DH. Thermal physiology and energetics in male desert hamsters (*Phodopus roborovskii*) during cold acclimation. *J Comp Physiol B*. 2011;181(1):91–103.
46. Goverse G, Molenaar R, Macia L, Tan J, Erkelens MN, Konijn T, et al. Diet-derived short chain fatty acids stimulate intestinal epithelial cells to induce mucosal tolerogenic dendritic cells. *J Immunol*. 2017;198(5):2172–81.
47. Rasmussen KE, Pedersen-Bjergaard S, Krogh M, Uglund HG, Gronhaug T. Development of a simple in-vial liquid-phase microextraction device for drag analysis compatible with capillary gas chromatography, capillary electrophoresis and high-performance liquid chromatography. *J Chromatogr A*. 2000;873(1):3–11.
48. Caporaso JG, Lauber CL, Walters WA, Berg-Lyons D, Huntley J, Fierer N, et al. Ultra-high-throughput microbial community analysis on the Illumina HiSeq and MiSeq platforms. *ISME J*. 2012;6(8):1621–4.
49. Magoc T, Salzberg SL. FLASH: fast length adjustment of short reads to improve genome assemblies. *Bioinformatics*. 2011;27(21):2957–63.
50. Caporaso JG, Kuczynski J, Stombaugh J, Bittinger K, Bushman FD, Costello EK, et al. QIIME allows analysis of high-throughput community sequencing data. *Nat Methods*. 2010;7(5):335–6.
51. Edgar RC. Search and clustering orders of magnitude faster than BLAST. *Bioinformatics*. 2010;26(19):2460–1.
52. Cole JR, Wang Q, Cardenas E, Fish J, Chai B, Farris RJ, et al. The ribosomal database project: improved alignments and new tools for rRNA analysis. *Nucleic Acids Res*. 2009;37(Database issue):D141–5.
53. Parks DH, Beiko RG. Identifying biologically relevant differences between metagenomic communities. *Bioinformatics*. 2010;26(6):715–21.
54. Segata N, Izard J, Waldron L, Gevers D, Miropolsky L, Garrett WS, et al. Metagenomic biomarker discovery and explanation. *Genome Biol*. 2011;12(6):R60.
55. McNab BK. The physiological ecology of vertebrates. Ithaca: Cornell Univ Press; 2002.
56. Li QF, Sun RY, Huang CX, Wang ZK, Liu XT, Hou JJ, et al. Cold adaptive thermogenesis in small mammals from different geographical zones of China. *Comp Biochem Physiol A*. 2001;129(4):949–61.
57. Wunder BA, Dobkin DS, Gettinger RD. Shifts of thermogenesis in the prairie vole (*Microtus ochrogaster*): strategies for survival in a seasonal environment. *Oecologia*. 1977;29(1):11–26.
58. Wang JM, Zhang YM, Wang DH. Seasonal regulation of energetics, serum concentrations of leptin, and uncoupling protein 1 content of brown adipose tissue in root voles (*Microtus oeconomus*) from the Qinghai-Tibetan plateau. *J Comp Physiol B*. 2006;176(7):663–71.
59. Gębczyński M. Social regulation of body temperature in the bank vole. *Acta Theriol Sin*. 1969;14:427–40.
60. Andrews RV, Phillips D, Makihara D. Metabolic and thermoregulatory consequences of social behaviors between *Microtus townsendii*. *Comp Biochem Physiol A*. 1987;87(2):345–8.
61. Scantlebury M, Bennett NC, Speakman JR, Pillay N, Schradin C. Huddling in groups leads to daily energy savings in free-living African four-striped grass mice, *Rhabdomys pumilio*. *Funct Ecol*. 2006;20(1):166–73.
62. Prychodko W. Effect of aggregation of laboratory mice (*Mus musculus*) on food-intake at different temperatures. *Ecology*. 1958;39(3):500–3.
63. Springer SD, Gregory PA, Barrett GW. Importance of social grouping on bioenergetics of the golden mouse *Ochrotomys nuttalli*. *J Mammal*. 1981; 62(3):628–30.
64. Kauffman AS, Paul MJ, Butler MP, Zucker I. Huddling, locomotor, and nest-building behaviors of furred and furless Siberian hamsters. *Physiol Behav*. 2003;79(2):247–56.
65. Wang D, Wang Z, Wang Y, Yang J. Seasonal changes of thermogenesis in Mongolian gerbils (*Meriones unguiculatus*) and Brandt's voles (*Microtus brandti*). *Comp Biochem Physiol A*. 2003;134:596.
66. Bennett AF, Ruben JA. Endothermy and activity in vertebrates. *Science*. 1979;206:649–54.
67. Kojima S, Alberts JR. Warmth from skin-to-skin contact with mother is essential for the acquisition of filial huddling preference in preweanling rats. *Dev Psychobiol*. 2011;53(8):813–27.
68. Fortin D, Gauthier G, Larochelle J. Body temperature and resting behavior of greater snow goose goslings in the high Arctic. *Condor*. 2000;102(1):163–71.
69. Gilbert C, Maho YL, Perret M, Ancel A. Body temperature changes induced by huddling in breeding male emperor penguins. *Am J Phys*. 2007;292(1):R176–85.
70. Glanville EJ, Seebacher F. Advantage to lower body temperatures for a small mammal (*Rattus fuscipes*) experiencing chronic cold. *J Mammal*. 2010;91(5):1197–204.
71. Zhang Z, Xu D, Wang L, Hao J, Wang J, Zhou X, et al. Convergent evolution of rumen microbiomes in high-altitude mammals. *Curr Biol*. 2016;25:1873–9.
72. Brinig MM, Lepp PW, Ouverney CC, Armitage GC, Relman DA. Prevalence of bacteria of division TM7 in human subgingival plaque and their association with disease. *Appl Environ Microb*. 2003;69(3):1687–94.
73. Jaeschke H, Schaarschmidt J, Eszlinger M, Huth S, Puttinger R, Rittinger O, et al. A newly discovered TSHR variant (L665F) associated with nonautoimmune hyperthyroidism in an Austrian family induces constitutive TSHR activation by steric repulsion between TM1 and TM7. *J Clin Endocr Metab*. 2014;99(10):E2051–E9.
74. Cho I, Yamanishi S, Cox L, Methe BA, Zavadil J, Li K, et al. Antibiotics in early life alter the murine colonic microbiome and adiposity. *Nature*. 2012; 488(7413):621–6.
75. Meehan CJ, Beiko RG. A phylogenomic view of ecological specialization in the Lachnospiraceae, a family of digestive tract-associated bacteria. *Genome Biol Evol*. 2014;6(3):703–13.
76. Fan WG, Huo GC, Li XM, Yang LJ, Duan CC, Wang TT, et al. Diversity of the intestinal microbiota in different patterns of feeding infants by Illumina high-throughput sequencing. *World J Microb Biotechnol*. 2013;29(12):2365–72.

77. Pedersen C, Gallagher E, Horton F, Ellis RJ, Ijaz UZ, Wu HH, et al. Host-microbiome interactions in human type 2 diabetes following prebiotic fibre (galacto-oligosaccharide) intake. *Br J Nutr*. 2016;116(11):1869–77.
78. Chayama Y, Ando L, Tamura Y, Miura M, Yamaguchi Y. Decreases in body temperature and body mass constitute pre-hibernation remodelling in the Syrian golden hamster, a facultative mammalian hibernator. *Roy Soc Open Sci*. 2016;3(4):160002.
79. Carey HV, Andrews MT, Martin SL. Mammalian hibernation: cellular and molecular responses to depressed metabolism and low temperature. *Physiol Rev*. 2003;83(4):1153–81.
80. Dill-McFarland KA, Neil KL, Zeng A, Sprenger RJ, Kurtz CC, Suen G, et al. Hibernation alters the diversity and composition of mucosa-associated bacteria while enhancing antimicrobial defence in the gut of 13-lined ground squirrels. *Mol Ecol*. 2014;23(18):4658–69.
81. Chi QS, Wan XR, Geiser F, Wang DH. Fasting-induced daily torpor in desert hamsters (*Phodopus roborovskii*). *Comp Biochem Physiol A*. 2016;199:71–7.
82. Szelenyi Z, Hummel Z, Szolcsanyi J, Davis JB. Daily body temperature rhythm and heat tolerance in TRPV1 knockout and capsaicin pretreated mice. *Eur J Neurosci*. 2004;19(5):1421–4.
83. Leone V, Gibbons SM, Martinez K, Hutchison AL, Huang EY, Cham CM, et al. Effects of diurnal variation of gut microbes and high-fat feeding on host circadian clock function and metabolism. *Cell Host Microbe*. 2015;17(5):681–9.
84. Thaiss CA, Levy M, Korem T, Dohnalova L, Shapiro H, Jaitin DA, et al. Microbiota diurnal rhythmicity programs host transcriptome oscillations. *Cell*. 2016;167(6):1495–510. e12
85. Bestion E, Jacob S, Zinger L, Di Gesu L, Richard M, White J, et al. Climate warming reduces gut microbiota diversity in a vertebrate ectotherm. *Nat Ecol Evol*. 2017;1:0161.
86. Obata Y, Pachnis V. The effect of microbiota and the immune system on the development and organization of the enteric nervous system. *Gastroenterology*. 2016;151(5):836–44.
87. Psichas A, Sleeth ML, Murphy KG, Brooks L, Bewick GA, Hanyaloglu AC, et al. The short chain fatty acid propionate stimulates GLP-1 and PYY secretion via free fatty acid receptor 2 in rodents. *Int J Obes*. 2015;39(3):424–9.
88. Perry RJ, Peng L, Barry NA, Cline GW, Zhang D, Cardone RL, et al. Acetate mediates a microbiome-brain-beta-cell axis to promote metabolic syndrome. *Nature*. 2016;534(7606):213–7.
89. Hong J, Jia Y, Pan S, Jia L, Li H, Han Z, et al. Butyrate alleviates high fat diet-induced obesity through activation of adiponectin-mediated pathway and stimulation of mitochondrial function in the skeletal muscle of mice. *Oncotarget*. 2016;7(35):56071–82.
90. Chambers ES, Viardot A, Psichas A, Morrison DJ, Murphy KG, Zac-Varghese SEK, et al. Effects of targeted delivery of propionate to the human colon on appetite regulation, body weight maintenance and adiposity in overweight adults. *Gut*. 2015;64(11):1744–54.
91. Hu JM, Kyrou I, Tan BK, Dimitriadis GK, Ramanjaneya M, Tripathi G, et al. Short-chain fatty acid acetate stimulates adipogenesis and mitochondrial biogenesis via GPR43 in brown adipocytes. *Endocrinology*. 2016;157:1881–94.
92. Li Z, Yi CX, Katiraei S, Kooijman S, Zhou E, Chung CK, et al. Butyrate reduces appetite and activates brown adipose tissue via the gut-brain neural circuit. *Gut*. 2017; <https://doi.org/10.1136/gutjnl-2017-314050>.

Ready to submit your research? Choose BMC and benefit from:

- fast, convenient online submission
- thorough peer review by experienced researchers in your field
- rapid publication on acceptance
- support for research data, including large and complex data types
- gold Open Access which fosters wider collaboration and increased citations
- maximum visibility for your research: over 100M website views per year

At BMC, research is always in progress.

Learn more biomedcentral.com/submissions

